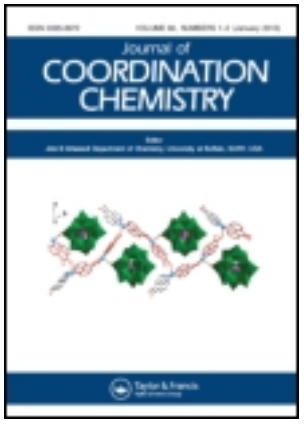

Journal of Coordination Chemistry
Publication details, including instructions for authors and subscription information:
http://www.tandfonline.com/loi/gcoo20

Vapor-assisted conversion synthesis of prototypical zeolitic imidazolate framework-8

Hui Zhang [a], Qi Shi [a], Xiaozhen Kang [a] & Jinxiang Dong [a]
[a] Research Institute of Special Chemicals, Taiyuan University of Technology, Shanxi, P.R. China
Accepted author version posted online: 22 Apr 2013.Published online: 29 May 2013.

To cite this article: Hui Zhang, Qi Shi, Xiaozhen Kang & Jinxiang Dong (2013) Vapor-assisted conversion synthesis of prototypical zeolitic imidazolate framework-8, Journal of Coordination Chemistry, 66:12, 2079-2090, DOI: 10.1080/00958972.2013.797966

To link to this article: http://dx.doi.org/10.1080/00958972.2013.797966

Journal of Coordination Chemistry, 2013
Vol. 66, No. 12, 2079–2090, http://dx.doi.org/10.1080/00958972.2013.797966

Vapor-assisted conversion synthesis of prototypical zeolitic imidazolate framework-8

HUI ZHANG, QI SHI*, XIAOZHEN KANG and JINXIANG DONG*

Research Institute of Special Chemicals, Taiyuan University of Technology, Shanxi, P.R. China

(*Received 6 September 2012; in final form 12 March 2013*)

ZIF-8 [$Zn(MIM)_2$, MIM = 2-methylimidazole] samples were synthesized by a vapor-assisted conversion method with *n*-heptane, methanol, and DMF, respectively. X-ray diffraction, thermogravimetric analysis, nitrogen (N_2) adsorption, Fourier transform infrared spectroscopy, and scanning electron microscopy were used to characterize the properties of the ZIF-8 samples. The particle sizes of the ZIF-8 samples synthesized with methanol, DMF, and *n*-heptane were 10–20, 60–90, and 30–50 μm, respectively. To our knowledge, this is the first time that ZIF-8 has been synthesized through vapor-assisted conversion with nonpolar *n*-heptane. For the ZIF-8 synthesis by this method, 0.5 mL of solvent was sufficient, greatly reducing the solvent dosage required compared with a traditional solvothermal method. In our study, on the crystallization of ZIF-8 synthesis by different liquid phases at 50 and 100 °C, we found that the transformation rate from the solid reagents to ZIF-8 phase with *n*-heptane was faster than that with methanol or DMF.

Keywords: *n*-Heptane; Vapor-assisted conversion method; Zeolitic imidazolate frameworks (ZIFs)

1. Introduction

Zeolitic imidazolate frameworks (ZIFs), one branch of metal-organic frameworks (MOFs), show the tunable pore size and chemical functionality of classical MOFs. The frameworks of ZIFs can be formulated as $T(IM)_2$ (T = tetrahedrally bonded metal ion; IM = imidazolate and its derivatives) and the T–IM–T angle is about 145°, coincident with the Si–O–Si angle commonly found in many zeolites [1]. Thus, ZIFs combine the advantages of both MOFs and zeolites. In other words, ZIFs have higher surface areas and greater structural diversity than zeolites and higher thermal, hydrothermal, and chemical stability than most MOFs [2]. Hence, ZIFs have attracted much attention in many applications such as gas adsorption [3–8], separation [4, 9–12], catalysis [13–16], and others [17–21].

Typical ZIFs were firstly synthesized through the liquid-phase diffusion method [22]. Then, the solvothermal method was introduced into ZIF synthesis and a number of ZIFs with specific or unknown zeolite topologies have been synthesized [23]. The vapor-assisted conversion method has been proven to be effective for synthesizing zeolites and zeolite membranes, as well as zeolite-like porous materials [24, 25]. In this method, the solvent

*Corresponding authors. Email: sq0085@link.tyut.edu.cn (Qi Shi); dongjinxiang@tyut.edu.cn (Jinxiang Dong)

(henceforth referred to as the liquid phase) and the solute (henceforth, the solid phase) are kept separated. Compared with the traditional solvothermal method, preparation with this method can greatly decrease the consumption of organic solvents in zeolite synthesis. Moreover, to our knowledge, the solvents used for ZIF synthesis are mainly polar, such as dimethylformamide (DMF), diethylformamide (DEF), and methanol. There have been no reports on the synthesis of ZIFs with nonpolar solvents.

In this paper, we synthesized prototypical ZIF-8 by the vapor-assisted conversion method with nonpolar *n*-heptane as well as polar DMF and methanol as the liquid phase. Afterwards, N_2 adsorption at 77 K, thermogravimetric analysis (TGA), Fourier transform infrared (FT-IR) spectroscopy, and scanning electron microscopy (SEM) were used to characterize the properties of the synthesized ZIF-8. To understand the crystallization process of ZIF-8 obtained with the different solvents, we followed the relationship between the product and reaction time ranging from 10 min to 24 h at 50 and 100 °C. We also studied the effects of the amount of the liquid phase and reaction ratio on the ZIF-8 synthesis.

2. Experimental

2.1. *Synthesis of ZIF-8*

The reagents employed were commercially available and used as received without purification. The set-up used in the experiment is illustrated in figure 1. In a typical synthesis, Zn $(OAc)_2 \cdot 2H_2O$ (0.11 g, 0.5 mmol) and 2-methylimidazole (MIM, 0.164 g, 2.0 mmol) were placed in a small Teflon® cup supported by a Teflon® holder. Each cup and holder was placed in a Teflon®-lined stainless steel autoclave. Either methanol, DMF or *n*-heptane (2.0 mL) was added to the bottom of each autoclave. The crystallization was then carried

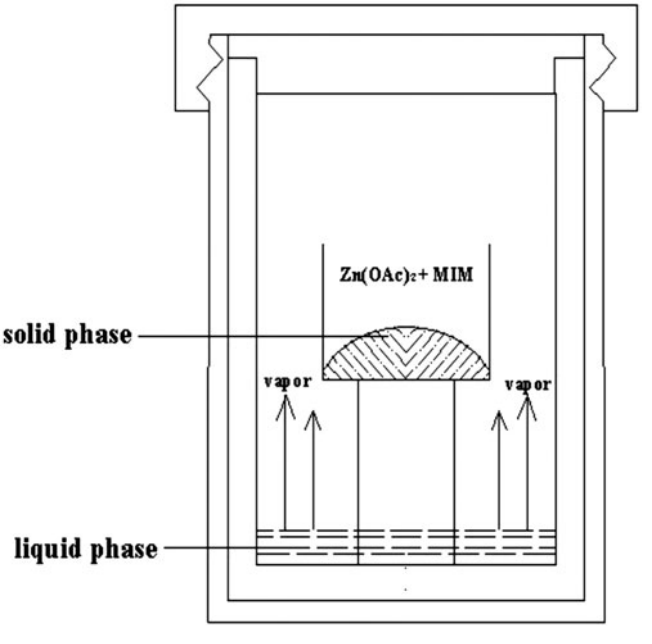

Figure 1. The reaction vessel used for ZIF-8 synthesis by the vapor-assisted conversion method.

out without stirring at 100 °C for 24 h. After cooling to room temperature, the solid products were separated by filtration and washed with ethanol. In order to study the effects of the reaction conditions on ZIF-8 synthesis, different $Zn(OAc)_2 \cdot 2H_2O$/MIM molar ratios (1 : 2, 1 : 4, 1 : 6, 1 : 8, and 1 : 10), reaction temperatures (50, 100, and 150 °C), reaction times (10 min to 5 days), and liquid-phase dosages (0.5, 1.0, 2.0, and 4.0 mL) were used.

2.2. *Characterization*

Powder XRD (PXRD) patterns were recorded on an X-ray diffractometer (MiniFlex II, Rigaku, Japan) at 30 kV and 15 mA using Cu Kα ($\lambda = 1.5418$ Å) radiation, with a scanning speed of 4° min^{-1}, a step size of 0.01° in 2θ, and scanning range from 3–40°. For N_2 adsorption, the activation of ZIF-8 was vitally important, so the samples were immersed in methanol (3 × 30 mL) for 3 days at room temperature and evacuated at 150 °C for 12 h. After pretreating the samples as above, N_2 adsorption was conducted on a Micromeritics ASAP 2020 sorptometer at 77 K. The mass of each sample used for N_2 adsorption was about 0.1 g, and the samples were degassed at 200 °C for 12 h. TGA was performed on a thermogravimetric (TG) analyzer (STA 409, NETZSCH, Germany). The temperature was increased at a rate of 10 °C min^{-1} from room temperature to 800 °C under a static air atmosphere. SEM micrographs were obtained with a scanning electron microscope (TM 3000, Hitachi, Japan). Infrared (IR) spectra from 4000–400 cm^{-1} were collected on a FT-IR spectrometer (IRAffinity-1, SHIMADZU, Japan) with KBr pellets. IR spectra were recorded on the samples before and after immersion in methanol.

3. Results and discussion

3.1. *Characterization results*

The PXRD patterns of ZIF-8 synthesized at 100 °C and for 24 h by the vapor-assisted conversion method with different liquid phases are shown in figure 2. Based on data in the

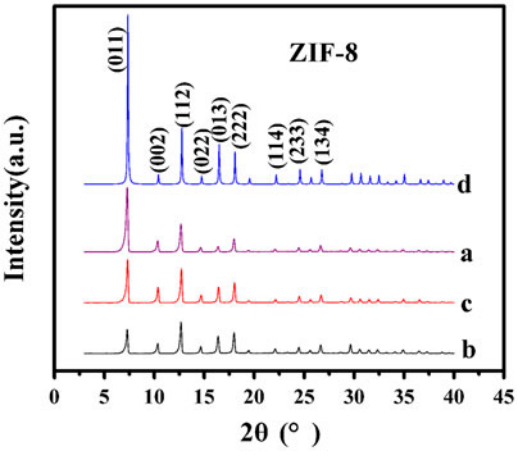

Figure 2. PXRD patterns of ZIF-8 synthesized by the vapor-assisted conversion method with different liquid phases: (a) methanol; (b) DMF; (c) *n*-heptane; (d) literature pattern [26].

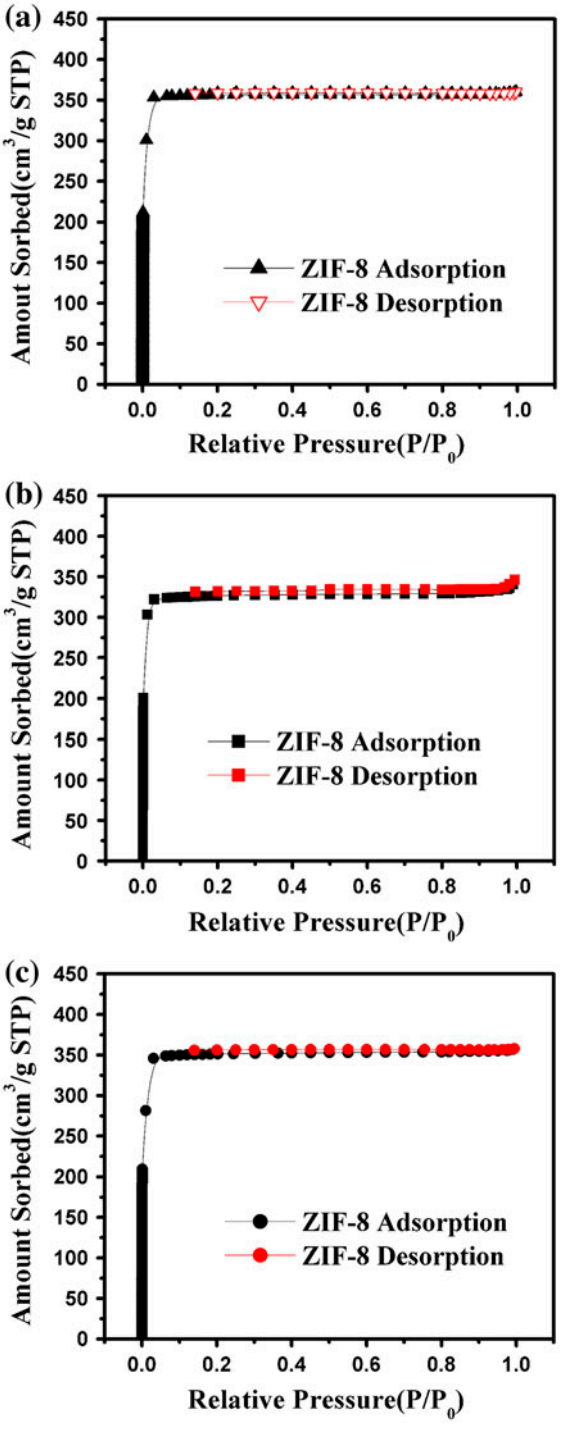

Figure 3. N_2 isotherms at 77 K for ZIF-8 samples synthesized by the vapor-assisted conversion method with different liquid phases: (a) methanol; (b) DMF; (c) *n*-heptane.

literature [26], high-order reflections (for example (0 1 1), (0 0 2) planes) for ZIF-8 are labeled in figure 2. The experimental PXRD patterns matched well with the published pattern except in terms of peak intensity, which means that ZIF-8 can be prepared with this method with methanol, DMF or *n*-heptane as the liquid phase.

Due to the difficulty in removal of DMF included in the ZIF-8 structure by heating, the as-synthesized ZIF-8 should be subjected to solvent-exchange before gas sorption analysis [2]. Figure 3 shows the N_2 adsorption/desorption isotherms at 77 K of the ZIF-8 samples synthesized with different liquid phases and after immersion in methanol. All the three isotherms are typically reversible type I isotherms, which revealed that the ZIF-8 samples were microporous. The BET (and Langmuir) surface areas for the samples synthesized with methanol, DMF, and *n*-heptane were 1186 (1555), 1089 (1428), and 1167 (1534) $m^2 g^{-1}$, respectively, while the micropore volumes were 0.54, 0.49, and 0.53 $cm^3 g^{-1}$, respectively. The obtained values are within the corresponding reported values [2, 21, 22, 27–30]. Differences between our values and the highest reported values can be explained by the different synthesis conditions and methods and the different treatment methods of the samples before N_2 adsorption. In our case, the treatment methods (such as the washing step [30] and the evacuation conditions) of the ZIF-8 samples may lead to the relatively low values.

The TG curves in figure 4 show some differences between the ZIF-8 samples prepared with different liquid phases. From the TG data for ZIF-8 synthesized with methanol, no noticeable mass loss was observed at temperatures up to 320 °C, at which point decomposition of the framework structure commenced. The solid residue (35 wt.%) obtained at the end of the TG analysis was consistent with ZnO (calculated, 35.8 wt.%). Thus, these results suggest that no solvent molecules were present in the cavities of the synthesized ZIF-8. This result is in the agreement with previous experimental results [12, 31]. The weight percentages of the remaining material for ZIF-8 synthesized with methanol and *n*-heptane were basically the same, so we can also infer that few *n*-heptane molecules were included in the as-synthesized framework. For ZIF-8 synthesized with DMF, there was about a 24 wt.% weight loss at 380 °C, and the weight percentage of the remaining material was about 28 wt.%, the same as reported [31]. The framework started to decompose rapidly after the temperature reached to 380 °C and collapsed completely by 550 °C. Thus,

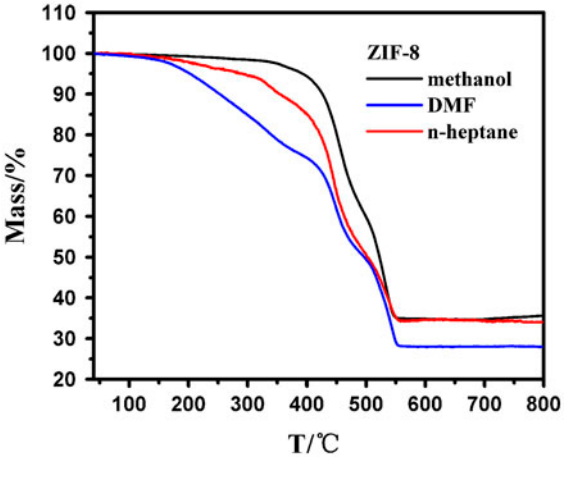

Figure 4. Thermogravimetric data for ZIF-8 synthesized with different liquid phases.

we can infer that some DMF was included in the framework, consistent with previous reports [2].

FT-IR is a useful method for identifying organic functional groups. Figures S1(a) and S1(c) show that there were no significant differences for the ZIF-8 samples synthesized with methanol and *n*-heptane before immersion in methanol, which proved that the solvents methanol and *n*-heptane were essentially not included in the framework of ZIF-8. In figure S1(b), a sharp band at 1685 cm^{-1}, a characteristic peak for –C=O, was observed. After immersion in methanol, this IR band had basically disappeared, which meant that the interstitial DMF molecules were exchanged out of the framework. This is more evidence of the existence of DMF within the as-synthesized ZIF-8 framework. In order to demonstrate the removal of DMF after immersion, TG data were collected (figure S2). After immersion in methanol, no noticeable mass loss was observed at temperatures up to 300 °C; in addition, the weight percentage of the remaining ZnO was again 35 wt.%, indicative of effective solvent-exchange.

Figure 5 shows that ZIF-8 crystals prepared with different liquid phases at 100 °C for 1 day had a typical rhombic dodecahedron shape with 12 exposed {1 1 0} faces [31]. From figure 5, we conclude that the size of ZIF-8 samples synthesized with *n*-heptane was 30–50 μm. The sizes of ZIF-8 samples synthesized with methanol and DMF were 10–20 and 60–90 μm, respectively. The ZIF-8 sample prepared by DMF had the largest size. There are many factors affecting the nucleation and growth of crystals, such as the

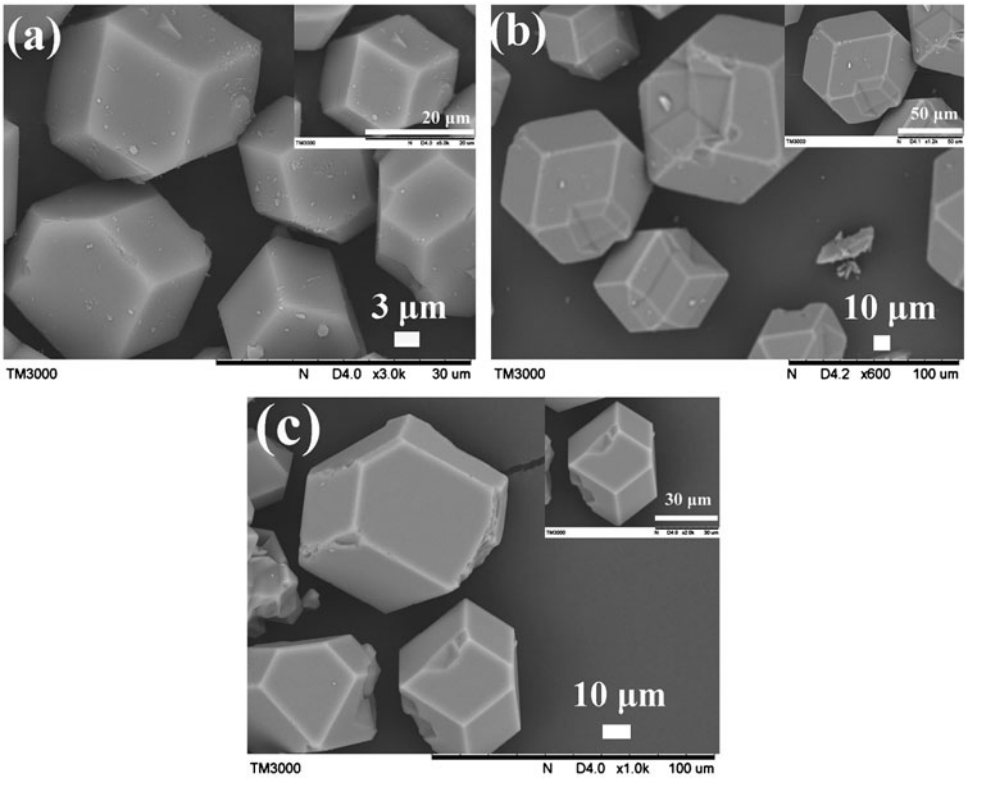

Figure 5. SEM images for ZIF-8 samples synthesized with different liquid phases: (a) methanol; (b) DMF; (c) *n*-heptane.

volatility and polarity of the solvent and the solubility of solute in solvent. In order to accurately explain the effect of the different liquid phases on crystal size, further detailed work needs to be done.

3.2. *The effect of the amount of liquid phase*

Different amounts of liquid phases were used to synthesize ZIF-8. Pure ZIF-8 can even be synthesized when 0.5 mL of the liquid phases were used (figure 6). This demonstrated that the required dosage of the liquid phase was greatly reduced by the vapor-assisted conversion method; only a small amount of solvent can trigger the reaction. It was found that 1.0 or 2.0 mL of solvent was the optimum dosage for ZIF-8 synthesis. Also, some solvent is left on the bottom of the reactor at the end of the reaction, which can be recycled for further syntheses, a remarkable characteristic.

3.3. *The effect of reaction ratio*

The effect of different $Zn(OAc)_2 \cdot 2H_2O$/MIM molar ratios on ZIF-8 synthesis has been studied at 100 °C and 24 h reaction time. As it is known, the theoretical molar ratio of

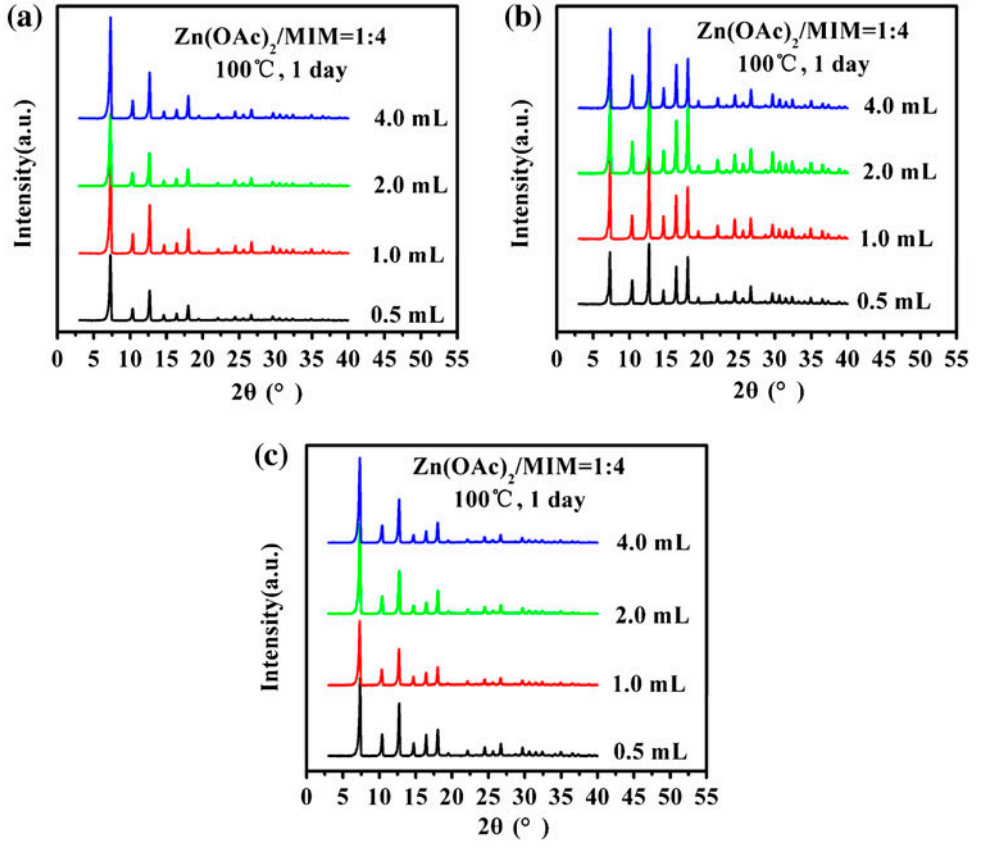

Figure 6. PXRD patterns of ZIF-8 synthesized with different amounts of liquid phases: (a) methanol; (b) DMF; (c) *n*-heptane.

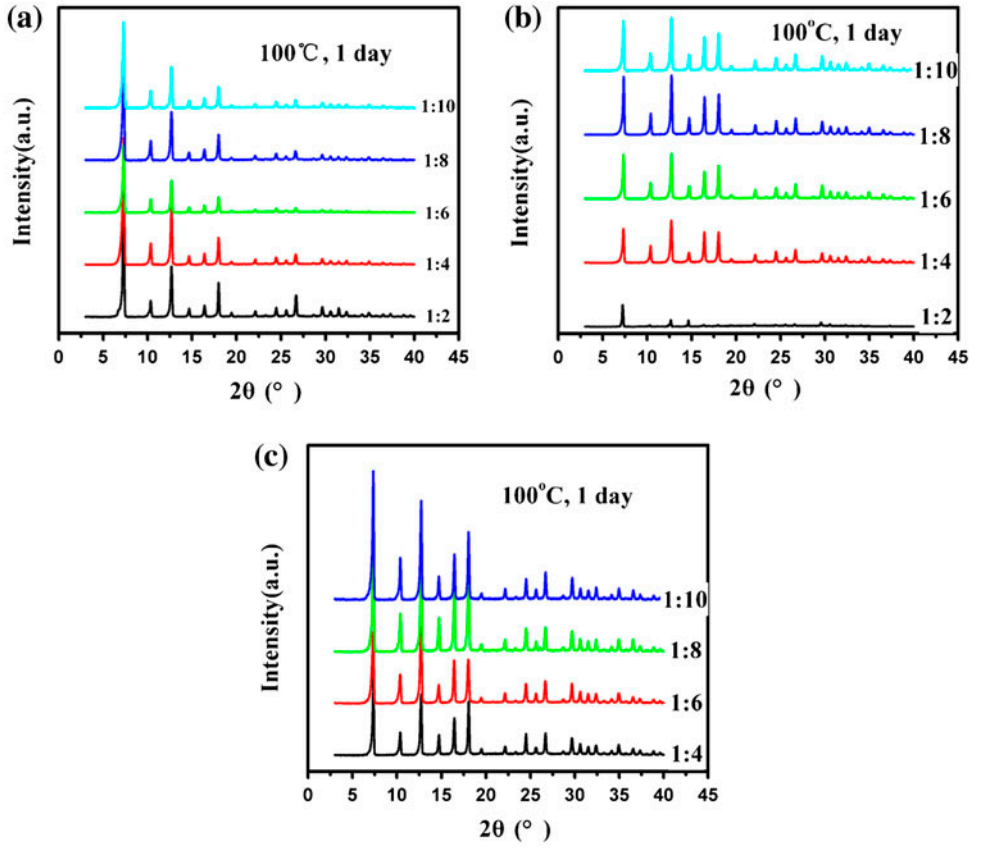

Figure 7. PXRD patterns of ZIF-8 synthesized with different $Zn(OAc)_2 \cdot 2H_2O$/MIM molar ratios and with different liquid phases: (a) methanol; (b) DMF; (c) *n*-heptane.

$Zn(OAc)_2 \cdot 2H_2O$/MIM for ZIF-8 synthesis is 1 : 2. However, practical synthetic methodology favors an excess of MIM for synthesizing ZIF-8. This can be illustrated by the PXRD patterns in figure 7. No ZIF-8, only an amorphous, ethanol-soluble material, was obtained when the reaction ratio was 1 : 2 and *n*-heptane was used as the liquid phase (figure S4).

3.4. *Study on the crystallization process of ZIF-8*

In order to explore the crystallization process of ZIF-8 synthesized with *n*-heptane, the relationship between product composition and reaction time ranging from 10 min to 24 h was determined at 50 °C (below the boiling point of *n*-heptane, 98.5 °C) and a 1 : 4 Zn $(OAc)_2 \cdot 2H_2O$/MIM molar ratio. Figure 8 shows the PXRD patterns of the products synthesized with *n*-heptane as a function of reaction time. When the reaction time was 30 min, only pure $Zn(OAc)_2$ was found (MIM was removed upon washing with ethanol, $Zn(OAc)_2$ was not). At longer reaction times, the relative intensities of the peaks for $Zn(OAc)_2$ decreased. At 3 h, weak diffraction peaks for ZIF-8 began to appear in the PXRD pattern. Pure ZIF-8 with *n*-heptane as the liquid phase was obtained after 12 h. For comparsion, we studied the crystallization process of ZIF-8 synthesized with methanol and DMF at 50 °C

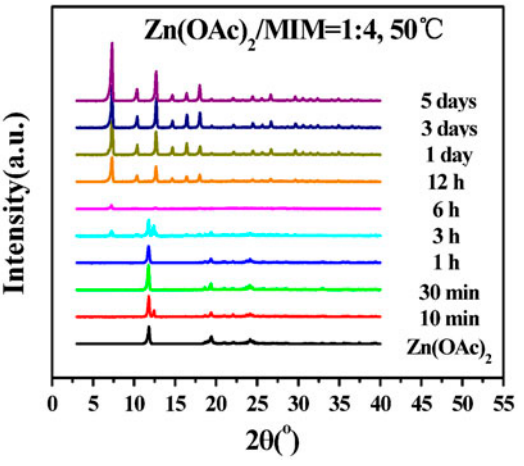

Figure 8. PXRD patterns of the products of ZIF-8 synthesis with *n*-heptane at 50 °C as a function of reaction time.

(figure S5). For ZIF-8 synthesis with methanol at 50 °C (below the boiling point of methanol, 64.8 °C), pure $Zn(OAc)_2$ was found after 1 h, but the pure ZIF-8 phase did not appear even after 24 h (figure S5(a)). No ZIF-8 was isolated even when the reaction time extended to 5 days. Figure S5(b) shows the PXRD patterns of ZIF-8 synthesized with DMF at 50 °C (below the boiling point of DMF: about 149 °C) as a function of reaction time. Pure $Zn(OAc)_2$ was present after 1 h. As the reaction time increased, the relative intensity of the $Zn(OAc)_2$ peaks decreased but a pure ZIF-8 phase did not appear within 24 h. Taking the strong structure-directing effect of DMF into consideration [1], we inferred that ZIF-8 could be synthesized with DMF at 50 °C when the reaction time was longer than 24 h, such as 3 or 5 days. As confirmed by experiments, pure ZIF-8 was prepared with DMF at 50 °C after 5 days (figure S5(b)).

As concluded from the above experiments, the rate of formation of ZIF-8 at 50 °C with *n*-heptane was faster than that with methanol or DMF. This phenomenon may be attributed to two factors. One, the nonpolarity of *n*-heptane and the similarity in hydrophobicity between *n*-heptane and ZIF-8 [32] may contribute to the solid-phase transformation as $Zn(OAc)_2$ and MIM are not easily dissolved in *n*-heptane. Two, the relative high volatility of *n*-heptane can easily generate enough vapor to trigger the solid-phase transformation. According to the Saturated Vapor Pressure data (table S1), the volatility of the three liquid phases at a given temperature is methanol > *n*-heptane > DMF.

For the ZIF-8 synthesis with methanol, the high volatility of methanol can easily generate enough vapor, and $Zn(OAc)_2$ and MIM are more easily dissolved in methanol than in *n*-heptane. However, the low temperature (50 °C) was unable to lead to the formation of ZIF-8 after 5 days. For the synthesis of ZIF-8 with DMF, the low volatility of DMF generated only a small amount of vapor, which led to a very slow formation rate of ZIF-8, as shown by the failure to obtain pure ZIF-8 with DMF at 50 °C within 24 h. However, due to the strong-directing effect of DMF, ZIF-8 was obtained when reaction time was extended to 5 days.

Similar experiments were also carried out at 100 °C. The PXRD patterns of ZIF-8 synthesized with the three liquid phases at 100 °C as a function of reaction time are shown in figures 9 and S6. Pure ZIF-8 was synthesized by *n*-heptane within 1.5 h (figure 9). ZIF-8

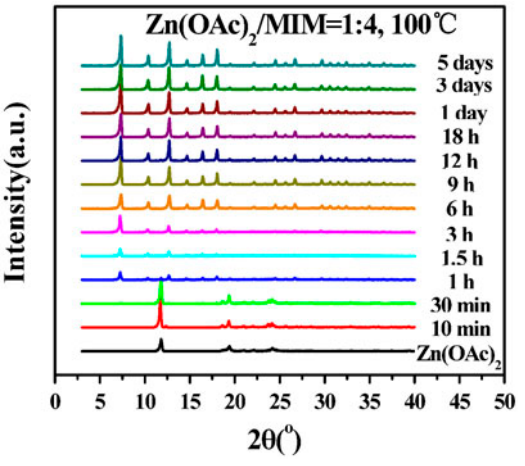

Figure 9. PXRD patterns of the products of ZIF-8 synthesis with *n*-heptane at 100 °C as a function of reaction time.

was prepared with methanol and DMF after 9 and 3 h, respectively (figure S6). At 100 °C, ZIF-8 can be synthesized with the three liquid phases, and the formation rate of ZIF-8 with *n*-heptane was still faster than that with methanol or DMF.

In our study on the crystallization process of ZIF-8, we found that the reaction time for obtaining pure ZIF-8 was greatly shortened at 100 °C compared with that at 50 °C, indicating that a relatively high temperature was good for synthesizing ZIF-8. Figure S7 shows the PXRD patterns of ZIF-8 synthesis at 50, 100, and 150 °C with different liquid phases after 24 h. In addition, the relative crystallinity of ZIF-8 synthesized at 100 °C with longer reaction times (3 or 5 days) was obviously better than that with a shorter time (6 h). We calculated the relative crystallinity [33] of ZIF-8 synthesized at 100 °C and different reaction times (figures S8-S10 and table S2) from the integrated area of the (0 1 1) plane, as quantified using the Origin software. Similar results which showed that long synthesis

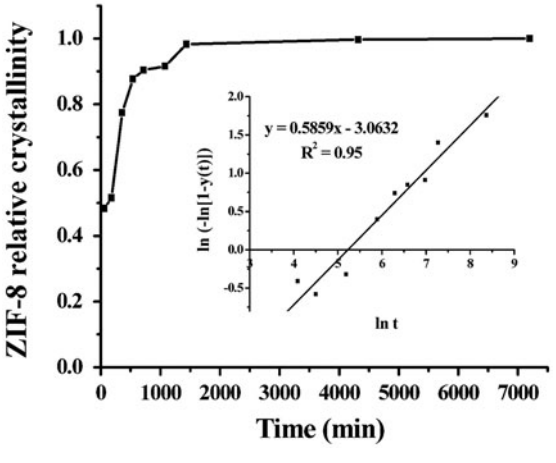

Figure 10. Crystallization rate curve of ZIF-8 synthesized at 100 °C with *n*-heptane. Inset shows the growth regime follows Avrami's kinetics.

times promote the complete crystallization of ZIF-8 have been published [26, 33]. Figure 10 shows the crystallization rate curve of ZIF-8 synthesized with *n*-heptane at 100 °C according to the calculated values in table S2. Interestingly, the formation kinetics followed Avrami's model (inset of figure 10) in the growth regime. Thus, the relative crystallinity of ZIF-8 as a function of time in this region can be expressed as $y = 1 - \exp(-kt^n)$, where k is a scaling constant and n is Avrami's constant [26]. The scaling constant k and Avrami's constant n can be obtained by the linear fit shown in the inset of figure 10. For ZIF-8 synthesis with *n*-heptane, $k = 0.047$ and $n \approx 0.59$. Although typical values of Avrami's constant n are in the range of 1–4, this constant can adopt different values, including fractional numbers < 1 [34]. Similar procedures were used to obtain values k and n for ZIF-8 synthesis with methanol and DMF (figures S11 and S12). Values of $n < 1$ have been typically attributed to both decreasing nucleation and growth rates as crystallization proceeds [26, 34]. A value of $n = 0.27$ has been reported for ZIF-8 [26].

4. Conclusion

Pure ZIF-8 samples were synthesized with methanol, DMF or *n*-heptane by a vapor-assisted conversion method. Through TGA and FT-IR analyses, we conclude that molecules of DMF were included in the framework, whereas little or no *n*-heptane or methanol was incorporated. This is the first time that ZIF-8 has been synthesized by the vapor-assisted method with nonpolar *n*-heptane. This finding enlarges the species of solvents that can be used for ZIFs synthesis, and we infer that other nonpolar solvents may be used to synthesize ZIFs. The BET (Langmuir) surface area and micropore volume of ZIF-8 synthesized with *n*-heptane were 1167 (1534) $m^2 g^{-1}$ and 0.53 $cm^3 g^{-1}$, respectively. The amount of liquid phase required for this method is much less than that needed for the solvothermal method, substantially reducing the waste of solvent, and unreacted solvents can be recycled in further syntheses. By exploring the crystallization of ZIF-8 synthesis with different liquid phases, we found that the transformation rate from the solid reagents to ZIF-8 with *n*-heptane was faster than that with methanol or DMF.

Supplementary materials

Figures of FT-IR spectra, TG data, low magnification SEM images, PXRD patterns of products synthesized with different molar ratios, reaction times, and temperatures, integrated areas of the (0 1 1) PXRD peak of ZIF-8 at different reaction times, crystallization rate curves, and determination of the Avrami k and n constants. Tables of Partial Saturated Vapor Pressure data and ZIF-8 relative crystallinity as a function of reaction time.

Acknowledgments

This work was supported by the National Natural Science Funds (Grant no. 51172153), Program for the Shanxi Province Foundation for Returness.

References

[1] Y.-Q. Tian, Y.-M. Zhao, Z.-X. Chen, G.-N. Zhang, L.-H. Weng, D.-Y. Zhao. *Chem. Eur. J.*, **13**, 4146 (2007).
[2] K.S. Park, Z. Ni, A.P. Côté, J.Y. Choi, R. Huang, F.J. Uribe-Romo, H.K. Chae, M. O'Keeffe, O.M. Yaghi. *Proc. Natl. Acad. Sci. USA*, **103**, 10186 (2006).

[3] A.R. Millward, O.M. Yaghi. *J. Am. Chem. Soc.*, **127**, 17998 (2005).
[4] R. Banerjee, A. Phan, B. Wang, C. Knobler, H. Furukawa, M. O'Keeffe, O.M. Yaghi. *Science*, **319**, 939 (2008).
[5] H. Wu, W. Zhou, T. Yildirim. *J. Am. Chem. Soc.*, **129**, 5314 (2007).
[6] L. Mu, B. Liu, H. Liu, Y. Yang, C. Sun, G. Chen. *J. Mater. Chem.*, **22**, 12246 (2012).
[7] A. Phan, C.J. Doonan, F.J. Uribe-Romo, C.B. Knobler, M. O'Keeffe, O.M. Yaghi. *Acc. Chem. Res.*, **43**, 58 (2010).
[8] Z. Zhang, S. Xian, H. Xi, H. Wang, Z. Li. *Chem. Eng. Sci.*, **66**, 4878 (2011).
[9] D. Britt, H. Furukawa, B. Wang, T.G. Glover, O.M. Yaghi. *Proc. Natl. Acad. Sci. USA*, **106**, 20637 (2009).
[10] S.R. Venna, M.A. Carreon. *J. Am. Chem. Soc.*, **132**, 76 (2010).
[11] K. Li, D.H. Olson, J. Seidel, T.J. Emge, H. Gong, H. Zeng, J. Li. *J. Am. Chem. Soc.*, **131**, 10368 (2009).
[12] H. Bux, F. Liang, Y. Li, J. Cravillon, M. Wiebcke, J. Caro. *J. Am. Chem. Soc.*, **131**, 16000 (2009).
[13] C. Chizallet, S. Lazare, D. Bazer-Bachi, F. Bonnier, V. Lecocq, E. Soyer, A.-A. Quoineaud, N. Bats. *J. Am. Chem. Soc.*, **132**, 12365 (2010).
[14] U.P.N. Tran, K.K.A. Le, N.T.S. Phan. *ACS Catal.*, **1**, 120 (2011).
[15] C.M. Miralda, E.E. Macias, M. Zhu, P. Ratnasamy, M.A. Carreon. *ACS Catal.*, **2**, 180 (2011).
[16] H.-L. Jiang, B. Liu, T. Akita, M. Haruta, H. Sakurai, Q. Xu. *J. Am. Chem. Soc.*, **131**, 11302 (2009).
[17] G. Lu, J.T. Hupp. *J. Am. Chem. Soc.*, **132**, 7832 (2010).
[18] C.-Y. Sun, C. Qin, X.-L. Wang, G.-S. Yang, K.-Z. Shao, Y.-Q. Lan, Z.-M. Su, P. Huang, C.-G. Wang, E.-B. Wang. *Dalton Trans.*, 6906 (2012).
[19] Y.-Q. Tian, C.-X. Cai, X.-M. Ren, C.-Y. Duan, Y. Xu, S. Gao, X.-Z. You. *Chem. Eur. J.*, **9**, 5673 (2003).
[20] S. Keskin, S. Kızılel. *Ind. Eng. Chem. Res.*, **50**, 1799 (2011).
[21] Q. Shi, Z. Chen, Z. Song, J. Li, J. Dong. *Angew. Chem. Int. Ed.*, **123**, 698 (2011).
[22] X.-C. Huang, Y.-Y. Lin, J.-P. Zhang, X.-M. Chen. *Angew. Chem. Int. Ed.*, **118**, 1587 (2006).
[23] B. Wang, A.P. Cote, H. Furukawa, M. O'Keeffe, O.M. Yaghi. *Nature*, **453**, 207 (2008).
[24] W. Xu, J. Dong, J. Li, J. Li, F. Wu. *J. Chem. Soc., Chem. Commun.*, 755 (1990).
[25] N. Nishiyama, T. Matsufuji, K. Ueyama, M. Matsukata. *Microporous Mater.*, **12**, 293 (1997).
[26] M. Zhu, S.R. Venna, J.B. Jasinski, M.A. Carreon. *Chem. Mater.*, **23**, 3590 (2011).
[27] Y. Pan, Y. Liu, G. Zeng, L. Zhao, Z. Lai. *Chem. Commun.*, **47**, 2071 (2011).
[28] A.F. Gross, E. Sherman, J.J. Vajo. *Dalton Trans.*, 5458 (2012).
[29] J. Cravillon, R. Nayuk, S. Springer, A. Feldhoff, K. Huber, M. Wiebcke. *Chem. Mater.*, **23**, 2130 (2011).
[30] A. Demessence, C. Boissiere, D. Grosso, P. Horcajada, C. Serre, G. Ferey, G.J.A.A. Soler-Illia, C. Sanchez. *J. Mater. Chem.*, **20**, 7676 (2010).
[31] J. Cravillon, S. Münzer, S.-J. Lohmeier, A. Feldhoff, K. Huber, M. Wiebcke. *Chem. Mater.*, **21**, 1410 (2009).
[32] P. Küsgens, M. Rose, I. Senkovska, H. Fröde, A. Henschel, S. Siegle, S. Kaskel. *Microporous Mesoporous Mater.*, **120**, 325 (2009).
[33] S.R. Venna, J.B. Jasinski, M.A. Carreon. *J. Am. Chem. Soc.*, **132**, 18030 (2010).
[34] T. Pradell, D. Crespo, N. Clavaguera, M.T. Clavaguera-Mora. *J. Phys. Condens. Matter*, **10**, 3833 (1998).